Correction of horizontal turbulence with nematic liquid crystal wavefront corrector

Zhaoliang Cao,[1,2] Quanquan Mu,[1,2] Lifa Hu,[1] Dayu Li, [1] Yonggang Liu,[1] Lu Jin[3], and Li Xuan[1,*]

[1]State Key Laboratory of Applied Optics, Changchun Institute of Optics, Fine Mechanics and Physics, Chinese Academy of Sciences, Changchun, Jilin, 130033, China
[2]Graduate School of the Chinese Academy of Sciences, Beijing, 100039, China
[3]School of Microelectronics & Solid-State Electronics, University of Electronic Science and Technology of China, Chengdu, 610054, China
[*]Corresponding author: xuanli1957@sina.com

To correct horizontal turbulences, a nematic liquid crystal wavefront corrector (NLC WFC) with a fast response is used. It can linearly modulate 2π radian at a wavelength of 633 nm. The closed-loop frequency of the adaptive optics system was originally only 12 Hz. Hence, a control system using the NLC WFC was developed, graphic processing units (GPUs) were used to compute the compensated wavefront, and the driving software for the NLC WFC was optimized. With these improvements, the closed loop frequency increased up to 60 Hz. Finally, the correction of a 500-m horizontal turbulence was performed with this fast adaptive system. After the correction, the averaged peak-to-valley (PV) and root-mean-square (RMS) values of the wavefront were reduced to 0.2λ and 0.06λ, respectively. The core of a fiber bundle is also resolved with a field angle of 0.68″. As the limit of the angular resolution of the telescope is 0.65″, the quasi-diffraction limited image is acquired with the closed-loop correction. It is shown that the NLC WFC has the ability to correct weak turbulences.

OCIS codes: (010.1080) Adaptive optics; (230.3720) Liquid-crystal devices; (010.1330) Atmospheric turbulence

References and links

1. L. Hu, L. Xuan, Y. Liu, Z. Cao, D. Li, and Q. Mu, "Phase-only liquid crystal spatial light modulator for wavefront correction with high precision," Opt. Express **12**, 6403-6409 (2004).
2. G. Love, "Wave-front correction and production of Zernike modes with a liquid-crystal spatial light modulator," Appl. Opt. **36**, 1517-1524 (1997).
3. F. Vargas-Martín and P Artal, "Phasor averaging for wavefront correction with liquid crystal spatial light modulators," Opt. Commun. **152**, 233-238 (1998).
4. S. Serati and J. Stockley, "Advances in liquid crystal based devices for wavefront control and beamsteering," Proc. SPIE **5894**, 58940K-1-58940K-13 (2005).
5. D. Dayton, J. Gonglewski, S. Restaino, and S. Browne, "MEMS adaptive optics for high resolution imaging of low Earth Orbit Satellites," Proc. SPIE **5490**, 1514-1525 (2004).
6. N. Konforti, E. Marom, and S. T. Wu, "Phase-only modulation with twisted nematic liquid crystal spatial light modulators,"Opt. Lett. **13,** 251-253(1988).
7. Q. Mu, Z. Cao, L. Hu, D. Li and L. Xuan**,** "Adaptive optics imaging system based on a high-resolution liquid crystal on silicon device," Opt. Express **14**, 8013-8018(2006).
8. Q. Mu, Z. Cao, D. Li, L. Hu, and L. Xuan**,** "Liquid crystal based adaptive optics system to compensate both low and high order aberrations in model eye," Opt. Express **15**, 1946-1953(2007).
9. D. C. Burns, I. Underwood, J. Gourlay, A. O'Hara, and D. G. Vass, "A 256×256 SRAM-XOR pixel ferroelectric liquid crystal over silicon spatial light modulator," Opt. Commun. **119**, 623-632 (1995).
10. M. A. A. Neil, M. J. Booth, and T. Wilson, "Dynamic wave-front generation for the characterization and testing of optical systems," Opt. Lett. **23**, 1849-1851 (1998).
11. S. R. Restaino, D. Dayton, S. Browne, J. Gonglewski, J. Baker, S. Rogers, S. McDermott, J. Gallegos, and M. Shilko, "On the use of dual frequency nematic material for adaptive optics systems: first results of a closed –loop experiment," Opt. Express **6**, 2-6 (2000).

#93137 - $15.00 USD Received 25 Feb 2008; revised 11 Apr 2008; accepted 23 Apr 2008; published 1 May 2008

12. D. Dayton, J. Gonglewski, and S. Restaino, et al., "Demonstration of new technology MEMS and liquid crystal adaptive optics on bright astronomical objects and satellites," Opt. Express **10**, 1508-1519 (2002).
13. D. Gu, B. Winker, B. Wen, D. Taber, A. Brackley, A. Wirth, M. Albanese, and F. Landers, "Wavefront control with a spatial light modulator containing dual frequency liquid crystal," Proc. SPIE **5553**, 68-82 (2004).
14. Z. Cao, L. Xuan, L. Hu, Y. Liu, Q. Mu, and D. Li, "Investigation of optical testing with a phase-only liquid crystal spatial light modulator," Opt. Express **13,** 1059-1065 (2005).
15. J. A. Jordan, Jr., P. M. Hirsch, L. B. Lesem, and D. L. Van Rooy, "Kinoform lenses," Appl. Opt. **9**, 1883-1887 (1970).
16. W. Chunhong, L. Mei, and L. Anna, "2900Hz High Speed Real Time Wavefront Processor," Opto-Electric Engineering Sup. **25,** 25-28 (1998) (In Chinese).
17. R. G. Belleman, J. Be′dorf, and S. F. Portegies Zwart, "High performance direct gravitational N-body simulations on graphics processing units II: An implementation in CUDA," New Astron. **13,** 103-112 (2008).
18. E. H. Wu, Y. Q. Liu, X. H. Liu, "An improved study of real-time fluid simulation on GPU," J. Computer Animation & Virtual World (CASA2004) **15**, 139-146 (2004).
19. http://developer.nvidia.com/object/cuda.html

1. Introduction

Liquid crystal devices are gaining importance and popularity in their use as wavefront correctors for adaptive optics [1–6]. Many researchers have used a nematic liquid crystal wavefront corrector (NLC WFC) to correct the distortions accompanying a low bandwidth [7, 8]. However, the slow response of the NLC material limits its application to astronomical observations. Hence, the use of dual-frequency and ferroelectric liquid crystal materials is considered to improve the switching frequency [9–12]. David Dayton, *et al.*, [12] have demonstrated the use of a dual-frequency liquid crystal adaptive optics system for observing satellites from ground-based telescopes. D. Gu, et al., [13] have fabricated a dual-frequency LC WFC with a frame rate of more than 500 Hz. However, due to the high driving voltages and complicated control methods, it is difficult to fabricate a dual-frequency LC WFC with millions active elements. The binary phase modulation of ferroelectric LC limits its application as a WFC. Currently, the response speed of the NLCs has been improved, which makes the NLC WFC feasible for correcting atmospheric turbulence. To the best of our knowledge, NLC WFCs have not been used for the correction of distortions in horizontal path turbulence until now.

In the present paper, we discuss the feasibility of using the NLC WFC in astronomical observations by carrying out the correction of a 500-m horizontal turbulence. As the NLC WFC has millions of pixels, wavefront reconstruction and data transfers can be time-consuming. A reduction in the operation time has been achieved to improve the closed-loop frequency of the control system.

2. Characteristics of NLC WFC

2.1 Measurement of phase modulation

A parallel aligned NLC WFC (PFP512, BNS) was used with the following dimensions: pixel pitch: 15 μm; 512 × 512 pixels; array size: 7.68 × 7.68 mm; filling factor: 83.4%; and zero-order diffraction efficiency: 61.5%. The phase modulation of the NLC WFC was measured with a ZYGO interferometer. A look-up table (LUT) was employed for the NLC WFC in order to obtain linear phase modulation. The phase modulation is shown in Fig. 1 as a function of the grey level. This indicates that the NLC WFC can linearly modulate 2π radians at a wavelength of 633 nm. As the NLC WFC can realize 2π radians of modulation, a phase-wrapping technique may be used to correct larger distortions [14, 15].

#93137 - $15.00 USD Received 25 Feb 2008; revised 11 Apr 2008; accepted 23 Apr 2008; published 1 May 2008

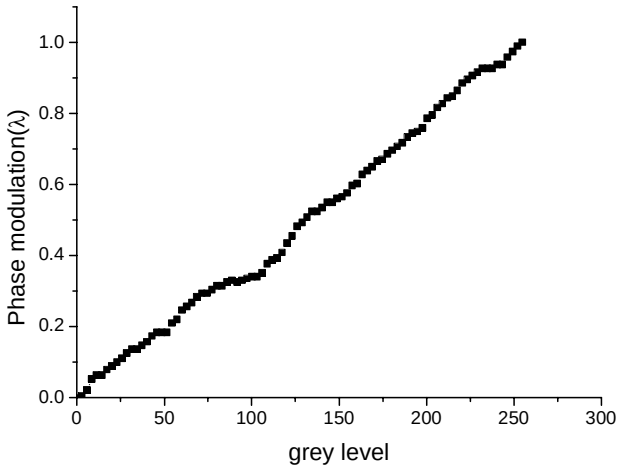

Fig. 1. Phase modulation as a function of grey level measured with ZYGO interferometer.

2.2 Response time of NLC WFC

The response time of the PFP512 was measured by Boulder Nonlinear Systems (BNS). The optical layout for the measurement is shown in Fig. 2. The first polarizer was aligned at 45°, and the second polarizer was crossed with respect to the first. A lens was used to focus the light onto the detector. The output of the detector was sent to an oscilloscope for measuring the response time. For the PFP512 from the LUT, the range of the grey levels is 0–127, and its corresponding voltage range is 1.14–2 V. Consequently, we must toggle all the pixels of the NLC WFC between the grey levels of 127 and 0. In the experiment, the NLC WFC is toggled between 1.14 V and 2 V. The measurement results are shown in Fig. 3. The lower curve represents the driving waveform, and the upper curve represents the response of the NLC WFC. It is seen that the response time is approximately 3.6 ms when the voltage changes from 1.14 V to 2 V. Therefore, the switching frequency of this NLC WFC can be increased up to 270 Hz.

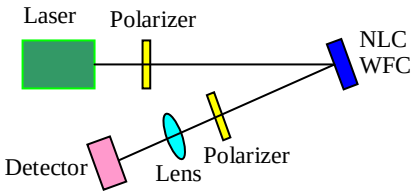

Fig. 2. Optical setup for measurement of the response time.

#93137 - $15.00 USD Received 25 Feb 2008; revised 11 Apr 2008; accepted 23 Apr 2008; published 1 May 2008

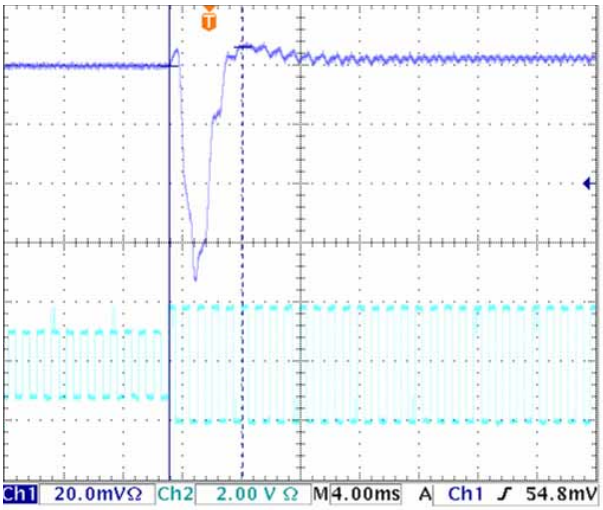

Fig. 3. Electrical-optical response of NLC WFC switching between 1.14V and 2V: the lower curve is the driving waveform; the upper is the electrical-optical response.

3. Time delay of the adaptive optics system

For the closed-loop control of the adaptive optics system, the wavefront sensor (WFS) first detects the distortions; the control device, a real-time computer (RTC), reconstructs the wavefront and transmits the conjugated signal to the NLC WFC; the NLC WFC corrects the distortions. In our adaptive optics system, a Shack-Hartmann WFS ShaH-1000 (Moscow State University) was used to measure the distortions. It has approximately 400 microlenses with apertures of 3 mm and an acquisition frequency of 500 Hz. The RTC is equipped with a Pentium D CPU (3.0 GHz), 2.0 GB Memory and a Windows XP Professional operating system.

The time delays of the closed loop control are shown in Fig. 4. As the CCD of the WFS has a frame rate of 500 Hz, both the exposure time and image output time are 2 ms. This indicates that calculations and data transmission result in significant time loss. Since the closed loop frequency was only 12 Hz, it cannot satisfactorily correct the turbulence.

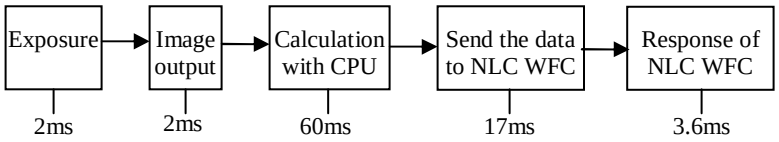

Fig. 4. Block diagram of the time delay of the control system.

4. Improvement of the closed loop frequency

4.1 Wavefront reconstruction with GPU

The calculation and reconstruction of the wavefront Zernike coefficients consumes almost no time with the CPU; however, since the NLC WFC has 512 × 512 actuators, the calculation of the grey map requires a longer time. Digital signal processors (DSPs) and parallel process techniques have been used to reduce the time of wavefront reconstruction [16]. However, with

#93137 - $15.00 USD Received 25 Feb 2008; revised 11 Apr 2008; accepted 23 Apr 2008; published 1 May 2008

this method, the control system becomes complicated and bulky. In this paper, a GPU is used to calculate the grey map so as to acquire powerful processing ability and a compact size.

GPUs have been used by many researchers for non-graphics computation [17, 18]. This technique has been applied to physics simulation, signal processing, computational biology, computational geometry, etc. Because the GPU is integrated in the graphic card, it is easy to control; hence, a single RTC is sufficient for the control and wavefront reconstruction in an adaptive control system. Furthermore, the GPU is a highly flexible and powerful processor with data-parallel processing and high arithmetic intensity. The computational ability of the GeForce 8800 Ultra graphic card can be up to 384 GFLOP/s. GeForce 8800 GTX outperforms the CPU of Intel Core2 X6800, which has a computational ability of 46.88 GFLOP/s, by a factor of 8.

In our RTC, the GeForce 8800 Ultra Graphic card is used to output video signals and to calculate the conjugated wavefront; its GPU supports 32-bit IEEE floating point numbers. Our GPU (768 MB memory; memory bandwidth: 103.7 GB/s; 612-MHz core clock) has 16 multiprocessors; each multiprocessor also has eight stream processors and shared memory.

The Compute Unified Device Architecture (CUDA) programming framework [19] allows the GPUs to be used as parallel data streaming processors with numerous processing units. Its application programming interface (API) is an extension of the 'C' programming language. GPUs can be viewed as coprocessors to the CPU or host. The CUDA can be used to control data transfers between the CPU and the GPU, and to calculate the data with stream processors. In a CUDA, a 'kernel' is used to execute data-parallel portions of an application; a kernel program is run in parallel on multiple threads. As shown in Fig. 5, the kernel is executed as a grid of thread blocks; each thread block is a set of threads that can cooperate with one another. However, two threads from two different blocks cannot cooperate. At the start of the calculation, the CPU sends control instructions to the kernel, which executes the calculation with the blocks and threads; upon completion of the calculation, the results are fed back to the host.

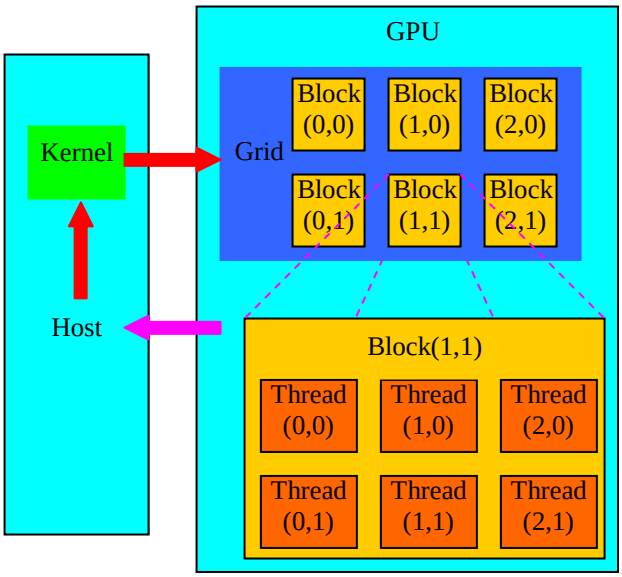

Fig. 5. Programming model of CUDA architecture.

For wavefront reconstruction applications, the computation cost is in direct ratio to the number of actuators. As our NLC WFC has 512 × 512 pixels, it needs a significantly longer computation time to obtain the driving voltages, i.e. the grey map, than a deformable mirror,

#93137 - $15.00 USD Received 25 Feb 2008; revised 11 Apr 2008; accepted 23 Apr 2008; published 1 May 2008

which has hundreds of actuators. Using DSP processors will be cumbersome since hundreds of them will be required to perform this calculation at computing speeds of the order of kHz. However, by using the GPU, a grey map with 512 × 512 points can be easily obtained at a high computing speed.

A kernel is used in order to obtain the grey map. The grid is divided into 32 × 32 blocks; each block contains 16 × 16 threads. Thus, 512 × 512 threads are used to calculate the reconstruction signal in parallel within 0.4 ms. Compared with the CPU, the time delay is drastically shortened. After the calculation is complete, the compensated data is fed back to the host within 1.6 ms.

4.2 Improvement of sending speed of data

The transmission of data to the NLC WFC results in a significant loss of time in the adaptive control system (shown in Fig. 4). The driving board of the NLC WFC with a PCI port is installed on the RTC. The host first transmits the compensated signal to the memory of this driving board; subsequently, the signal is transferred to the DAC (digital-analog converter) to be converted to an analog signal, which is then transmitted to the display panel. Since the electronic refresh rate of PFP512 can be up to 6 kHz, the time delay of the NLC WFC is mainly caused by transmitting data to the memory of the driving board. The PCI port of our host supports a transfer rate of 133 MB/s. Consequently, the ideal transfer time of 512 × 512 bytes can be reduced to 2 ms. However, the test results indicated a lag of 17 ms, which we assume is possibly caused by the incompatible driving software. With our improvement of the driving software, this time delay has been reduced to 7 ms. Further improvements are being made by BNS.

With the decrease in the time delay, the closed loop frequency has been increased to 60 Hz, which is sufficient for correcting weak turbulences.

5. Closed loop correction experiment of 500 meter horizontal turbulence

5.1 Optical layout

With the optimal control system, an adaptive correction experiment was performed to compensate the distortion of the 500-m horizontal turbulence. The optical layout is shown in Fig. 6. A white light was outputted with a fiber bundle. The fiber bundle was placed near the focal plane of the spherical mirror to simulate an infinite object located 500 m away. A 250-mm-aperture telescope was used to observe the simulated object in our laboratory; an adaptive optics system was positioned immediately behind the telescope to correct the distortions.

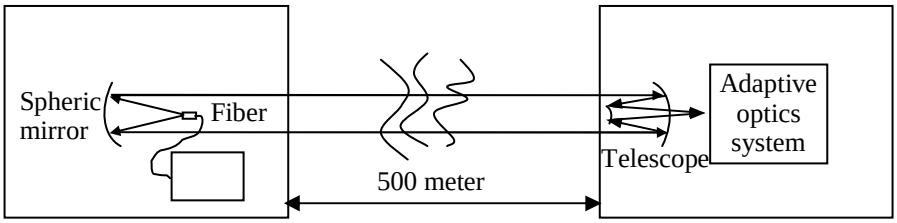

Fig. 6. Optical layout of the simulated infinite object and the observation.

The optical setup of the adaptive optics system is shown in Fig. 7. The light emerging from the telescope was collimated by lens L1, reflected by a tip-tilt mirror, and converted to polarized monochromatic light after transiting through the polarizer and narrowband colored filter. This collimated beam was zoomed in by L2 and L3, reflected by the NLC WFC and mirror, and directed to the beam splitter. The light beam was split into two by the beam splitter—one beam was captured by the CCD camera, and the other was used to measure the distortions.

#93137 - $15.00 USD Received 25 Feb 2008; revised 11 Apr 2008; accepted 23 Apr 2008; published 1 May 2008

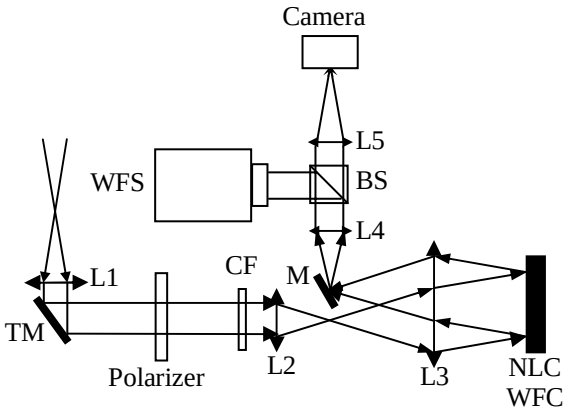

Fig. 7. Optical setup of adaptive optics system: L1 to L5, lenses, TM and CF represent tip-tilt mirror and narrowband colored filter respectively, BS, beam splitter, M is the mirror.

5.2 Experiment

The adaptive optics system is composed of WFS, RTC, tip-tilt mirror and an NLC WFC. An EM-CCD camera (DV897, Andor) is used to obtain the image of the fiber bundle. It has 512 × 512 pixels and an acquisition frequency of 34 Hz. A tip-tilt mirror (S-330, PI) with a resonant frequency of 2.4 kHz is used. The fiber bundle is composed of lots of fibers, and the diameter of each core of the fiber is 25 μm. The aperture of the whole fiber bundle is 1 mm. In order to obtain a suitable field angle of the core of the fiber, the fiber bundle is moved apart from the focus plane of the spheric mirror to produce the magnified virtual image. The field angle of the virtual image of the fiber bundle and the core of the fiber are 27″ and 0.68″, respectively.

Correction of 500-meter horizontal path turbulence was performed at the afternoon, Jan. 3, 2008. Before the correction, the average PV and RMS of the wavefront were 15.8λ (λ = 633 nm) and 4.1λ, respectively (Fig. 8(a)). A gain of 0.7 was selected in the closed-loop control software. While the closed-loop correction was performed, the RTC sent the tilt of the compensated wavefront to the tip-tilt mirror and high-order aberrations to the NLC WFC. After the closed-loop correction, the PV and RMS of the wavefront were reduced to 0.2λ and 0.06λ, respectively (Fig. 8(b)). The images of the fiber bundle are shown in Fig. 9. The core of

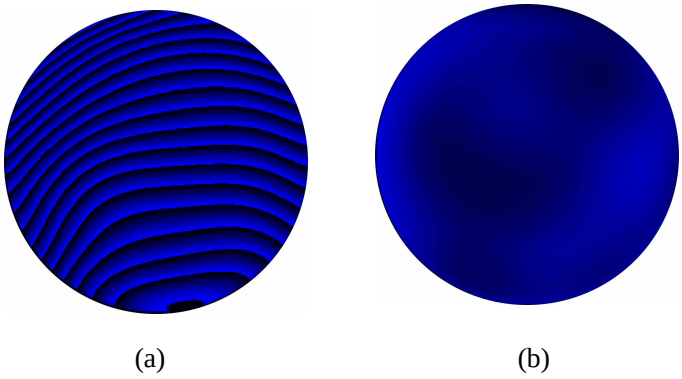

Fig. 8. Representative wavefront with fringe mode: (a) distorted; (b) corrected.

#93137 - $15.00 USD Received 25 Feb 2008; revised 11 Apr 2008; accepted 23 Apr 2008; published 1 May 2008

the fiber with a field angle of 0.68″ can be resolved with the adaptive correction. Since the limit of the angular resolution for our telescope was 0.64″, the quasi-diffraction limit was achieved. This indicates that the NLC WFC used in this improved control system is capable of correcting turbulences.

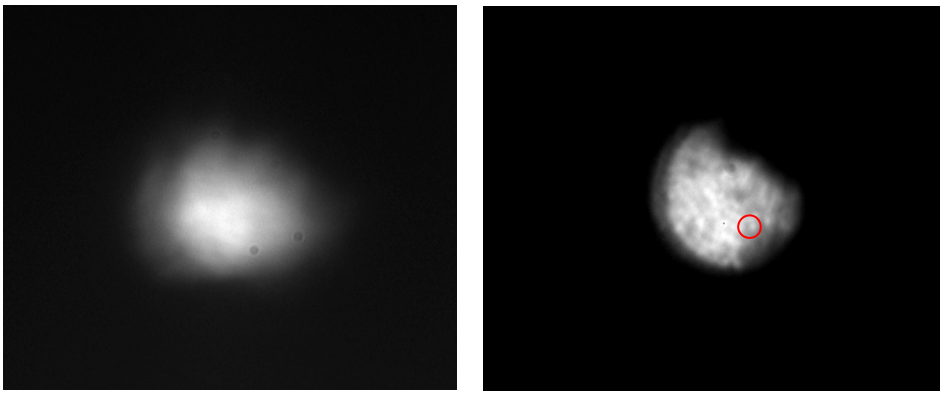

(a) (b)

Fig. 9. Images of the fiber bundle: (a) before correction; (b) after correction, the core of fiber bundle can be resolved in the red circle (2.72MB).

6. Conclusions

A NLC WFC used to correct the distortions in turbulence is investigated in this paper. In order to compensate for the turbulence, the control system must have a high closed-loop frequency. GPUs are used to calculate the compensated signal with a reduced time delay. As compared with a CPU, the time delay in the GPU calculation is decreased from 60 ms to 0.4 ms. The speed of data transfers between the host and the driving board is increased with optimal driving software. By using the GPU and optimal driving software, the closed loop frequency of the control system can be increased up to 60 Hz. Thus, it is possible to correct weak turbulences with this optimal control system.

The closed loop correction of a 500-m horizontal turbulence was performed with the fast-response NLC WFC. A white light source with a fiber bundle output and spherical mirror were used to simulate an infinite object located at a distance of 500 m. A telescope was used to observe the object, and the distortion in the turbulence was corrected with the adaptive optics system. While the closed-loop correction was performed, the core of the fiber bundle was resolved with a field angle of 0.68″; it is approximately equal to the limit of angular resolution of our telescope, and a quasi-diffraction limited image was obtained with the adaptive correction.

The results show that with an improvement in the closed loop frequency, the NLC WFC is feasible for correcting atmospheric turbulence. In the future, we intend to employ the NLC WFC to correct the mid-strength turbulence with a faster response NLC material and an advanced electric port.

Acknowledgments

Thanks to the help of Kelly Gregorak and Steve Serati (BNS) for measuring the response time of the PFP512. This work is supported by National Natural Science Foundation (No. 60736042, No. 60578035, No. 50473040).

#93137 - $15.00 USD Received 25 Feb 2008; revised 11 Apr 2008; accepted 23 Apr 2008; published 1 May 2008